
Design Considerations for a ^3He Refrigerator for Space Applications

Peter Kittel and Andres F. Rodriguez

FOR REFERENCE

NOT TO BE TAKEN FROM THIS ROOM

July 1984

LIBRARY COPY

1324

LYNGLEY RESEARCH
LIBRARY 1984
HAMPTON, VIRGINIA



National Aeronautics and
Space Administration



NF00829

Design Considerations for a ^3He Refrigerator for Space Applications

Peter Kittel

Andres F. Rodriguez, Ames Research Center, Moffett Field, California



National Aeronautics and
Space Administration

Ames Research Center
Moffett Field California 94035

N84-28001^H

DESIGN CONSIDERATIONS FOR A ^3He REFRIGERATOR FOR SPACE APPLICATIONS

Peter Kittel and Andres F. Rodriguez*

Ames Research Center

SUMMARY

The low temperature provided by ^3He refrigerators (0.3-3 K) have useful space applications. However, the low temperatures and the low surface tension of ^3He require special design considerations. These considerations include the need for small pores to contain the liquid in a matrix, the effects of bubble nucleation and growth, and the effects of the thermal conductivity within the matrix. These design considerations are discussed here along with an analysis of a possible confinement system.

SYMBOLS

a	acceleration
B_o	Bond number
B_1	$B_o / \rho h$
E_J	ejection number
E_1	$E_J r / \dot{Q}h$
F_a	$\rho \ell V_a$; force due to acceleration
F_p	force due to a pressure difference
F_s	force due to surface tension
F_t	force due to surface tension gradients
g	gravitational acceleration
h	height of liquid
h	Planck constant
k	Boltzmann constant
K_e	effective conductance
K_ℓ	conductance of liquid

*Permanent address: Department of Physics, University of the Pacific, Stockton, CA 95211.

K_m	conductance of matrix
L	latent heat
n	number of capillaries
N	number of liquid molecules
P	pressure
P_s	$F_s/\pi r^2$; pressure due to surface tension
ΔP	pressure difference
\dot{Q}	heat flux
\dot{Q}_p	total heat flux
r	radius
R	gas constant
t	hold time
T	temperature
T_c	condensation temperature
T_o	operating temperature
T_s	superheat
T_{sat}	saturation temperature
ΔT	temperature difference
V	volume
x	distance in the direction of a
α	rh
β	$\dot{Q}h/r$
ε	mass fraction lost during pump-down
κ_e	effective conductivity
κ_l	liquid conductivity
κ_m	matrix conductivity
η	volume void fraction
ρ_l	liquid density

ρ_v vapor density

σ surface tension

INTRODUCTION

The development of a space-compatible ^3He refrigerator would provide a significant improvement in several areas of research such as IR astronomy and the study of critical phenomena in quantum fluids (refs. 1 and 2). ^3He can produce refrigeration by evaporative cooling from 3.2 K (its critical point) to about 0.3 K. The lower limit is set by the vapor pressure and the system pumping speed.

While ^3He refrigeration has been used for a number of years in laboratories (refs. 3 and 4), on balloons (ref. 5), in aircraft (ref. 6), and in spin-stabilized sounding rockets (ref. 7), it has yet to be used in the low-gravity environment of space. Unlike ^4He , which was used in IRAS (ref. 8), ^3He is not a superfluid at these temperatures and cannot be contained by the fountain pressure generated by a temperature gradient.

A proposed ^3He refrigerator is shown in figure 1. While this is not the only possible configuration, this design will be used here as a reference in discussing the major features that are also common to other designs. This design consists of an adsorption pump, two heat switches, and a pot. The pot, the pump, and the interconnecting tubing form a sealed system that need be filled with ^3He only once. The heat switches connect the refrigerator to heat sinks whose temperatures are indicated in the figure. The refrigeration cycle starts with the system below 10 K. The pot switch is closed and the pump switch is opened. The adsorption pump is then heated to drive out the ^3He gas which condenses in the pot. When the condensation is complete, the heater is turned off and the switches are reversed. The pump cools, then readsobs the gas, causing evaporative cooling in the pot. When the pot runs dry, the cycle can be repeated.

Variations of this type of refrigerator have been used in the past whenever gravity or centrifugal force ensures that the liquid remains in the pot. The purpose of this paper is to discuss various aspects of containing the ^3He in space. If the pot is filled with a porous material the liquid ^3He can be contained by capillary attraction. Although surface tension methods have been used for controlling other fluids in space, the low temperatures and low surface tension of ^3He require special considerations. The use of capillary confinement in a ^3He refrigerator was first suggested by Ostermeier (ref. 9). Since then, Ennis (ref. 10) has demonstrated condensation, confinement, and useful refrigeration of both ^4He and ^3He in an inverted geometry. In many ways the inverted operation is a more severe test than a zero-gravity operation.

The main concerns with capillary confinement are whether the vapor can be condensed into the porous matrix without leaving large voids, and whether the liquid can be evaporated from the sponge without forming bubbles that would expel liquid. Expelled liquid would reduce the quantity of liquid available for cooling.

These concerns are discussed in the following sections, followed by a model of a proposed refrigeration system. The porous matrix will be modeled as a cluster of smooth cylindrical capillaries. These capillaries will be assumed to be parallel

to any acceleration of the refrigerator. Although real accelerations can occur in any direction, accelerations parallel to the capillary axis produce the largest effect. Deficiencies in this model will be discussed.

We would like to acknowledge the support of the NASA Office of Aeronautics and Space Technology.

CAPILLARY CONFINEMENT

The porous matrix serves two functions during the refrigeration cycle. It provides a place for the vapor to condense during the condensation phase, and it retains the liquid during the evaporation phase.

In order for the vapor to condense, several conditions must exist. The part of the system which is in contact with the vapor must be at a temperature below the critical temperature of the gas, and the pressure in the system must be greater than the corresponding vapor pressure. If these conditions are met, condensation will occur. If several areas are cold enough for condensation to occur, the condensation can be expected to occur preferentially at the coldest point. This effect is due to the vapor pressure decreasing and the surface tension increasing with decreasing temperature. Both the vapor pressure gradient and the surface tension gradient provide forces that drive the condensed liquid to the coldest point (cold spot) in the system. Thus, at the end of the condensation phase, all of the liquid will be condensed at the coldest point unless there is some other force, such as gravity, to drive the fluid elsewhere.

If the cold spot is a porous matrix, the condensation is enhanced because the surface tension is increased by the small size of the pores, and because the increased surface area increases the condensation rate. However, there may be a difficulty when using a porous matrix — that the condensation might take place only on the outside of the matrix, leaving voids in the interior. However, experiments by Donnelly (ref. 11) and Ennis (ref. 10) have not demonstrated this effect. They showed that the condensed liquid substantially fills the matrix.

In a spacecraft, the porous matrix must hold the liquid against any lateral accelerations. This is required during both the condensation and evaporation phases of the refrigeration cycle. These accelerations can, in general, occur in any direction and can be of variable magnitude. The effect of the acceleration forces is best described in terms of the Bond number, B_o (refs. 12 and 13). The Bond number is the ratio of the acceleration forces to the surface tension forces:

$$B_o = \frac{F_a}{F_s} = \frac{\rho_l arh}{2\sigma} \quad (1)$$

where we have assumed that the liquid wets the capillary wall with a contact angle of 0° ; so the cosine term that normally appears in the expression for the surface tension force can be ignored. This assumption is valid for ${}^3\text{He}$ (ref. 9) and will be used throughout this paper. If $B_o > 1$, the acceleration forces dominate, and if $B_o < 1$, the surface tension forces dominate. Thus, to retain the fluid, the matrix must be selected such that the stability condition, $B_o \ll 1$ is met for all expected accelerations. Since ρ_l and σ are properties of the refrigerant, and a is determined by the environment, the designer is free to choose only r and h . This restriction can be emphasized by separating B_o into two factors:

$$B_0 = \alpha B_1 \quad (2)$$

where $B_1 = \rho_\ell a/2\sigma$ gives the system properties and $\alpha = rh$ gives the design parameters. The stability condition can now be written as $\alpha \ll 1/B_1$. Since B_1 is a function of temperature, the stability condition must be evaluated over the whole operating temperature range, which is the range from the condensation temperature to the evaporation temperature. For the case in which $a = 9.8$ m/sec (1 g), the function $1/B_1$ for ^3He is shown in figure 2. For the curve in figure 2, the area below the curve is the stable region. For many applications, the accelerations can occur in any direction. Thus h must be the maximum dimension of the matrix from an open pore. This would lead one to think that the largest possible volume would be a sphere of radius h . However, the matrix is not floating free; rather it is almost entirely contained. The only opening is in the vent tube (fig. 3) and no part of the matrix can be a distance greater than h from the opening of the tube. Thus the greatest volume is a sphere of radius h . From the stability condition ($\alpha \ll 1/B_1$), it is readily seen that the smaller r is, the greater h can be; and thus the more liquid that can be held.

BUBBLE DYNAMICS

The porous matrix must not only confine the liquid during the condensation phase, but also during the evaporation phase. Bubbles that form during evaporation tend to expand. At first they will expand radially until they block the capillary. If the bubble expands past this point, it will displace and eventually expel liquid (ref. 14). Since the expelled liquid will not produce any useful cooling in the system, it is desirable to prevent the expulsion. This problem can be broken down into several aspects, starting with the initial formation of the bubbles, then their growth and movement within the capillaries. This process will be discussed in this section along with effects of real nonidealized porous matrices.

In a porous matrix, with its large irregular surface, bubbles will form by inhomogeneous nucleation at nucleation sites on the interface (refs. 15 and 16). Bubbles will form when the liquid temperature, T , is raised sufficiently above the saturation temperature, T_{sat} (ref. 17). The quantity ($T_s = T - T_{\text{sat}}$) is called the superheat. The amount of superheat required for nucleation depends on the surface properties of the interface. While it is difficult to predict this superheat exactly, an estimate can be made. Bald (ref. 16) derived an expression:

$$T_s \approx \frac{RT^2}{L} \ln \left\{ 1 + \frac{1}{P} \left(\frac{\rho_\ell}{\rho_\ell - \rho_v} \right) \left[\frac{16\pi\sigma^3}{3kT \ln(6N^2/3kT/h)} \right]^{1/2} \right\} \quad (3)$$

This function is shown in figure 4 as a function of temperature for ^3He for 1 mole of liquid.

Bubble formation can be prevented if the temperature gradients in the fluid are kept small and the superheat is never reached. These limitations require the effective thermal conductance K_e across the fluid to be large. In other words, the combined conductances of the matrix and the fluid must be considered between the heat source (where nucleation is most likely to occur) and the fluid's free surface (where evaporative cooling occurs). If the heat flow is rectilinear, then

$$K_e = K_m + K_l \quad (4)$$

where K_m and K_l are the thermal conductances of the matrix and the liquid, respectively. $\Delta T = Q/K_e$ gives the temperature drop across the system which must be less than the superheat. Thus for the system to be stable against the formation of bubbles, the following relation must hold:

$$\dot{Q}/K_e < T_s \quad (5)$$

This formula requires that K_e be large. Since K_l is set by the properties of ^3He , only K_m is a free parameter. A high-conductance matrix, such as copper, will give the best stability. The area-to-length ratios in K_m and K_l are also important. Because the conductivity of copper is considerably higher than ^3He , thick-walled capillaries will be more stable than thin-walled ones.

If we consider the heat flux into a single capillary of radius r and height h , then equation (5) can be expressed in terms of an equivalent conductivity κ_e where $K_e = \kappa_e \pi r^2/h$:

$$\frac{h}{r^2} \ll \frac{\kappa_e \pi T_s}{\dot{Q}} \quad (6)$$

(The equivalent conductivity can also be written in terms of the liquid and matrix conductivities, κ_l and κ_m , respectively, and the void fraction of the matrix: $\kappa_e = \kappa_l + \kappa_m (1 - \eta)/\eta$.)

If a bubble does form, it will be free to move within the liquid. In the absence of gravity, which gives rise to buoyancy, the only force available to move a bubble comes from surface tension gradients. Such motion is called Marangoni flow (ref. 18). The surface tension gradients are the result of temperature gradients and the temperature dependence of the surface tension. The surface tension of ^3He as a function of temperature is shown in figure 5. Young et al. showed that the buoyancy of a bubble will balance the Marangoni effect when

$$\frac{d\sigma}{dT} \frac{dT}{dx} = \frac{2\sigma_l gr}{3} \quad (7)$$

Since this balance occurs when the surface tension gradient force, F_t , is equal to F_a for $a = g$, F_t can be deduced:

$$F_t = \pi r^2 \frac{d\sigma}{dT} \frac{dT}{dx} \quad (8)$$

Thus the bubble tends to move toward the higher temperature; i.e., toward the heat source and away from the free surface of the liquid which is being evaporatively cooled.

Since the bubble most likely forms near the heat source, it will not move far, if at all. Furthermore, at low temperatures $d\sigma/dT$ approaches zero as does F_t . Thus at the operating temperature there will be no force to move a bubble. At higher temperatures there is another effect that prevents the bubbles from moving. At temperatures at which there is a substantial vapor pressure, the bubble acts like

a heat pipe (ref. 19). Vapor is evaporated from the hot side of the bubble and is condensed on the cold side. This increases the thermal conductivity of the bubble. The temperature gradient across the bubble is reduced, thus reducing F_t .

We have seen that once formed a bubble is not likely to move; it can only grow. Any growth must be accompanied by the displacement and eventual expulsion of liquid. This effect can be prevented if the growth of the bubbles can be controlled. To illustrate this, we will consider a bubble blocking an otherwise full capillary (fig. 6). There are two forces acting on the liquid. One, F_p , is the force due to the pressure difference, ΔP , across the liquid:

$$F_p = \pi r^2 \Delta P \quad (9)$$

The bubble's formation and growth is the result of a heat influx into the bubble. This results in a temperature gradient through the liquid. If quasi-static process is assumed where the vapor in the bubble and the vapor outside the capillary are in thermal equilibrium with their respective liquid interfaces, then equation (9) can be written as

$$F_p = \pi r^2 \frac{dP}{dT} \bigg|_{svp} \Delta T \quad (10)$$

The derivative, dP/dT , is evaluated along the saturated vapor pressure curve. This can be done in terms of the Clausius-Clapeyron equation (ref. 20):

$$\frac{dP}{dT} \bigg|_{svp} = \rho_v L/T \quad (11)$$

The ΔT in equation (10) can be expressed in terms of the equivalent thermal conductance, K_e :

$$\Delta T = \dot{Q}/K_e \quad (12)$$

where $K_e = K_m + K_l$ and \dot{Q} is the heat flux per capillary. As before $K_e = \kappa_e \tau r^2/h$. Using equations (11) and (12), equation (10) can be written as

$$F_p = \frac{\dot{Q} h \rho_v L}{\kappa_e T} \quad (13)$$

The other force acting on the liquid is the surface tension force:

$$F_s = 2\pi r \sigma \quad (14)$$

To aid in determining which of the two forces dominates, we will define an ejection number, E_j , as the ratio of F_p to F_s :

$$E_j = \frac{\dot{Q} h \rho_v L}{2\pi r \kappa_e \sigma T} \quad (15)$$

If $E_j < 1$, the surface tension force will dominate and the system will be stable against this form of expulsion. The expulsion number may be written as $E_j = \beta E_1$ where

$$E_1 = \frac{\rho_v L}{2\pi\sigma k_e T} \quad (16)$$

contains the system properties and

$$\beta = \dot{Q}h/r \quad (17)$$

contains the design parameters. The stability condition now becomes $\beta < 1/E_1$. A plot of $1/E_1$ as a function of temperature is shown in figure 7 for ${}^3\text{He}$ in a 50% copper matrix. This figure shows the regions of stability and instability.

A real matrix is not likely to be composed of smooth cylindrical capillaries but rather of irregular interconnected passages. The effect of the interconnections will be to increase the system's stability. The pressure in the bubble will be opposed by the surface tension of many pores. The pressure difference across the liquid is found by combining equations (9) and (13):

$$\Delta P = \frac{\dot{Q}h\rho_v L}{\pi r^2 k_e T} \quad (18)$$

The pressure due to the surface tension at n pores is

$$P_s = \frac{nF_s}{\pi r^2} = \frac{2n\sigma}{r} \quad (19)$$

Thus the $E_j = \Delta P/P_s$ is decreased by a factor of $1/n$, increasing the stability of the system.

APPLICATION

In this section we will discuss how the above considerations can be applied to the design of a refrigerator. To illustrate, we will consider a hypothetical refrigerator for cooling an IR detector. The refrigerator requirements are shown in table 1. We will assume that the liquid chamber is a sphere (fig. 3) with a volume $V = 4\pi h^3/3$. Since the capillary device is used both to contain the liquid and to conduct heat to the liquid-vapor interface, the entire volume will be filled with a high-conductivity matrix such as copper. For our example, we will assume that the void fraction is $\eta = 0.5$. Since the condensation occurs at T_c , a fraction, ϵ , of the liquid will be lost in pumping down to T_o . Furthermore, the volume of liquid will change because of the density change between T_c and T_o . After pump-down, a volume of liquid of $\dot{Q}_p t / L \rho_\ell$ must remain to meet the hold time requirement. Thus the volume of the liquid chamber must be

$$V \geq \frac{1}{\eta(1 - \epsilon)} \frac{\dot{Q}_p t}{L \rho_\ell(T_c)} \quad (20)$$

or

$$h \geq \left[\frac{3}{4\pi\eta(1-\epsilon)} \frac{\dot{Q}_p t}{L\rho_e(T_c)} \right]^{1/3} \quad (21)$$

For our example, these are $V \geq 7.8 \text{ cm}^3$ and $h \geq 1.2 \text{ cm}$.

Bond number considerations lead to another restriction on the chamber specifications. This is the requirement that $\alpha \ll 1/B_1$, over the entire operating range (T_c to T_o). We must use the smallest value of $1/B_1$ over this range. Since $1/B_1$ decreases with increasing temperature (fig. 2), the minimum occurs at T_c . Thus we have the restriction that

$$rh \ll 1/B_1(T_c) \quad (22)$$

where B_1 is evaluated at the peak expected acceleration. In our example the requirement becomes $rh \ll 2 \times 10^{-6} \text{ m}^2$.

A third restriction arises from the desire to avoid bubble nucleation. Equation (6) gives an expression for h/r in terms of the heat flux per capillary. To convert this to an expression in terms of $\dot{Q}_p = n\dot{Q}$, we must first estimate the total number of capillaries in the system. One such estimate is the ratio of the void volume to the volume of a single capillary:

$$n = \eta V / \pi r^2 h = 4\eta h^2 / 3r^2 \quad (23)$$

Substituting this into equation (6) gives

$$h > \frac{3\dot{Q}_p}{4n\pi k_e T_c s} \quad (24)$$

For our example this gives $h > 0.7 \text{ mm}$. Since this is so much less than the previous constraint on h (eq. 20), it may be ignored.

The last restriction comes from consideration of the ejection number. Again we must consider the entire temperature range. In this case $1/E_1$ decreases with increasing temperature (fig. 7), so its minimum value occurs at T_c . With this consideration, and again taking into account the number of capillaries in the system, the restriction that $\dot{Q}h/r < 1/E_1$ becomes

$$r/h < \frac{4n}{3\dot{Q}_p E_1(T_c)} \quad (25)$$

For our example this is $r/h < 0.02$.

The restrictions due to hold time, Bond number, and ejection number are shown in figure 8. As can be seen in the figure, there is a region of $r-h$ space in which a stable refrigerator could be designed. The curve for ejection criterion was calculated assuming noninterconnecting capillaries. If interconnecting capillaries are used, then this curve would move to the right and down, increasing the stable region. The figure shows the case for a single capillary. In practice, n will be the number of capillaries exposed to the pump-out tube.

CONCLUSION

It is feasible to design a ^3He refrigerator that will operate in the low-gravity environment of space where accelerations can occur in random directions. The key to the design is to fill the liquid chamber with a high-conductivity porous material such as sintered copper. The pores allow surface tension forces to contain the liquid while the conductivity ensures that the vaporization occurs at the surface of the matrix rather than internally. The matrix also provides a favorable place for condensation to occur and suppresses bubble nucleation and movement.

REFERENCES

1. Kittel, P.: Refrigeration Below 1 K in Space. *Physica*, vol. 108B, Aug. 1981, pp. 1115-1118.
2. Kittel, P.: Sub-Kelvin Temperatures in Space. *Adv. Cryo. Eng.*, vol. 27, 1982, pp. 745-749.
3. Chanin, G.; and Torre, J. P.: A Portable ^3He Cryostat for Space Applications. *Proc. Sixth Int. Cryo. Eng. Conf.*, IPC Science and Technology Press, 1977, pp. 96-98.
4. Kittel, P.; and Brooks, W. F.: Demountable Self-contained ^3He Refrigerator. *Adv. Cryo. Eng.*, vol. 27, 1982, pp. 727-734.
5. Woody, D. P.; and Richards, P. L.: Spectrum of the Cosmic Background Radiation. *Phys. Rev. Lett.*, vol. 42, Apr. 1979, pp. 925-929.
6. Radostitz, J. V.; Nolt, I. G.; Kittel, P.; and Donnelly, R. J.: Portable ^3He Detector Cryostat for the Far Infrared. *Rev. Sci. Instrum.*, vol. 49, Jan. 1978, pp. 86-88.
7. Gush, H.: Rocket Measurement of the Cosmic Background Submillimeter Spectrum. *Proc. Space Helium Dewar Conference* (to be published, U. of Alabama Press, 1984).
8. Urbach, A. R.; and Mason, P. V.: IRAS Cryogenic System Flight Performance Report. *Adv. Cryo. Eng.*, vol. 29, 1984, pp. 651-660.
9. Ostermeier, R. M.; Nolt, I. G.; and Radostitz, J. V.: Capillary Confinement of Cryogens for Refrigeration and Liquid Control in Space - I. Theory. *Cryogenics*, vol. 18, Feb. 1978, pp. 83-86.
10. Ennis, D. J.; Kittel, P.; Brooks, W. A.; Miller, A.; and Spivak, A. L.: A ^3He Refrigerator Employing Capillary Confinement of Liquid Cryogen. *Refrigeration for Cryogenic Sensors*, NASA CP-2287, 1983, pp. 405-417.
11. Donnelly, R. J.; Kittel, P.; Ostermeier, R. M.; Radostitz, J. V.; Lee, B. R.; and Cooper, J. C.: A Study of Confinement and Heat Transfer Properties of Cryogens, Final Report, NASA Grant NSG-2208, 1979.
12. Satterlee, H. M.; and Reynolds, W. C.: The Dynamics of the Free Surface in Cylindrical Containers Under Strong Capillary and Weak Gravity Conditions. Report LG-2, Mechanical Engineering Dept., Stanford University, 1964.
13. Alexander, G. E.; Barksdale, T. R.; Hise, R. E.; Lunden, K. C.; and Paynter, H. L.: Experimental Investigations of Capillary Propellant Control Devices for Low Gravity Environments, vol. II, Final Report, NASA Contract NAS8-21259, Martin Marietta Corp., 1970.
14. Labuntzov, D.; Evdokimov, O. P.; Tishin, I. V., and Ul'ianov, A. F.: Analytical Investigation of the Boiling Process in Small Diameter Tubes. *Mashinostroenie*, vol. 7, 1970, pp. 68-73.

15. Smith, R. V.: The Influence of Surface Characteristics on the Boiling of Cryogenic Fluids. *Trans. ASME. J. of Eng. for Indust.*, vol. 91, Nov. 1969, pp. 1217-1221.
16. Bald, W. B.: Bubble Nucleation at Real Surfaces with no Pre-existing Gaseous Phase, *Dept. of Engineering Report N-75-29279*, University of Oxford, 1975.
17. Kottowski, H. M.: The Mechanism of Nucleation, Superheating and Reducing Effects on the Activation Energy of Nucleation. *Prog. Heat and Mass Transfer*, vol. 7, 1973, pp. 299-324.
18. McGrew, J. L.; Rehm, T. L.; and Griskey, R. G.: The Effect of Temperature Induced Surface Tension Gradients on Bubble Mechanics. *App. Sci. Res.*, vol. 29, June 1974, pp. 195-210.
19. Young, N. O.; Goldstein, J. S.; and Block, M. J.: The Motion of Bubbles in Vertical Temperature Gradient. *J. Fluid Mech.*, vol. 6, Oct. 1959, pp. 350-356.
20. Reif, F.: Fundamentals of Statistical and Thermal Physics. McGraw-Hill, 1965, pp. 304-306.

TABLE 1.- REFRIGERATOR REQUIREMENTS

Parameter	Symbol	Value
Condensation temperature	T_c	2 K
Operating temperature	T_o	0.3 K
Hold time	t	54 ks
Refrigeration power ^a	\dot{Q}_p	40 μ W
Peak acceleration	a	0.1 g

^aIncludes parasitic loads.

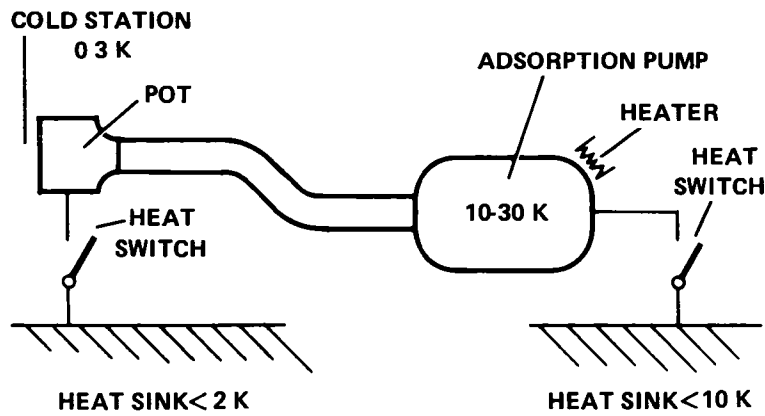


Figure 1.- A zero-gravity ^3He refrigerator showing the principal components.

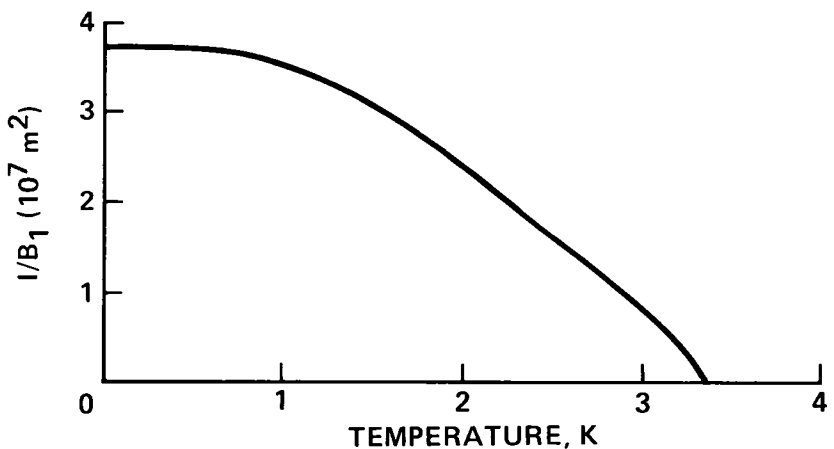


Figure 2.- Plot of $1/B_1$ as a function of temperature for ^3He for the case in which the acceleration is 9.8 m/sec. The region below the curve is the region in which surface tension forces dominate.

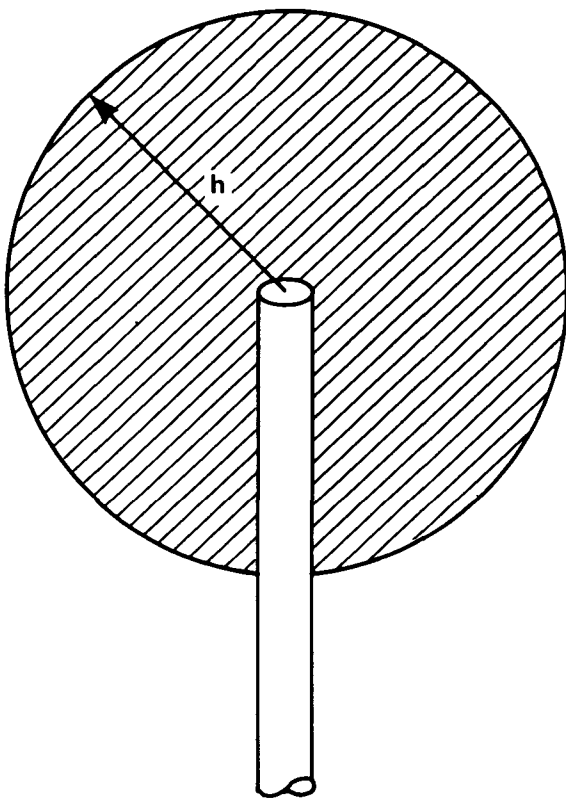


Figure 3.- The arrangement that allows the greatest volume of enclosed fluid. The exit tube penetrates to the center of a spherical cavity. The cavity is filled with the porous matrix.

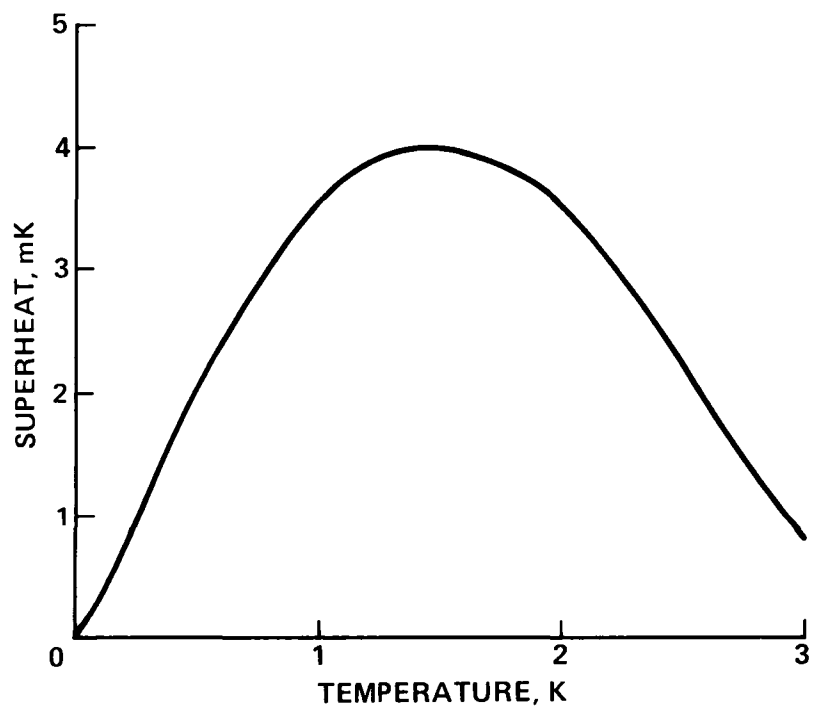


Figure 4.- Plot of the superheat in ${}^3\text{He}$ as a function of temperature.

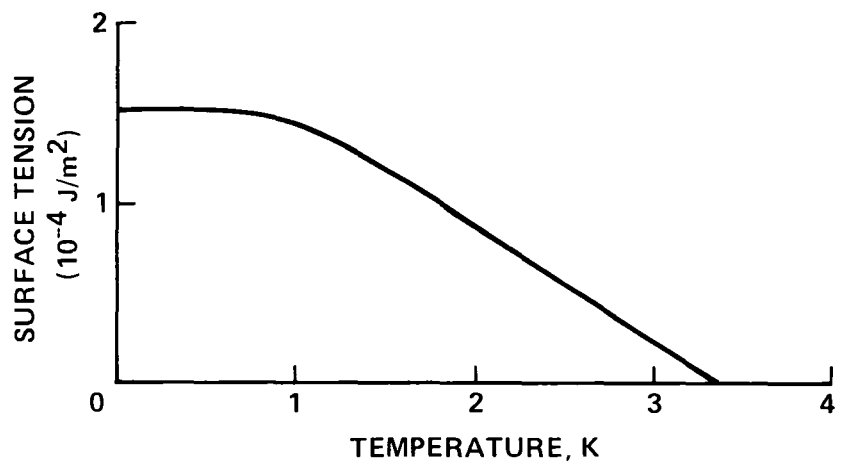


Figure 5.- Plot of the surface tension of ${}^3\text{He}$ as a function of temperature.

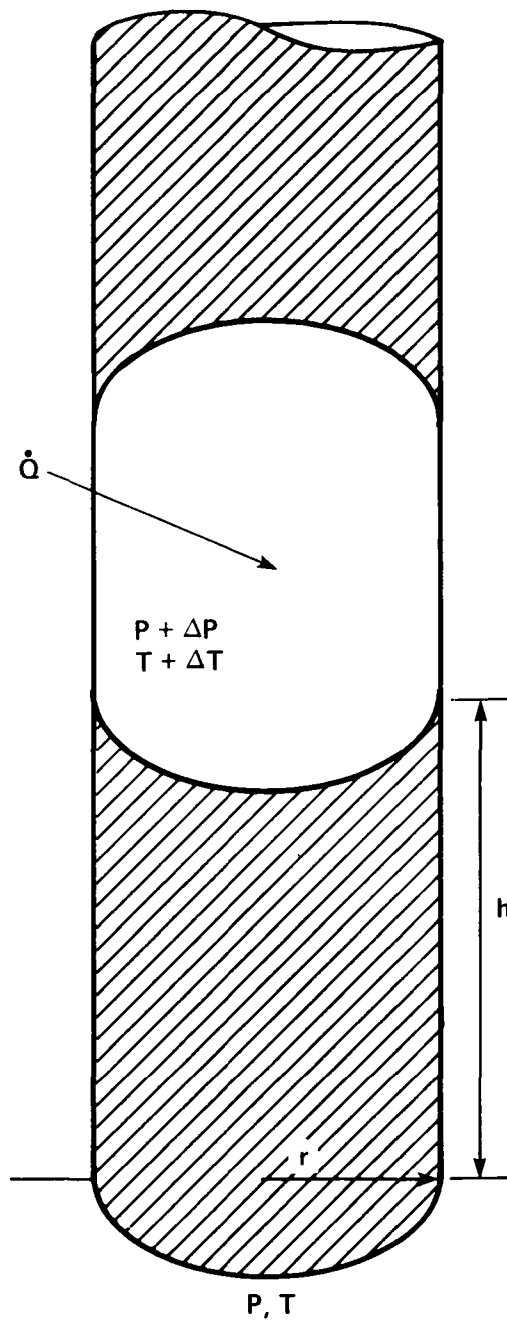


Figure 6.- A vapor bubble blocking an otherwise full capillary. The capillary has a radius of r . A column of liquid of height h separates the bubble from free space. A temperature difference of ΔT and a pressure difference of ΔP are across the liquid column. There is a heat flux of \dot{Q} into the bubble.

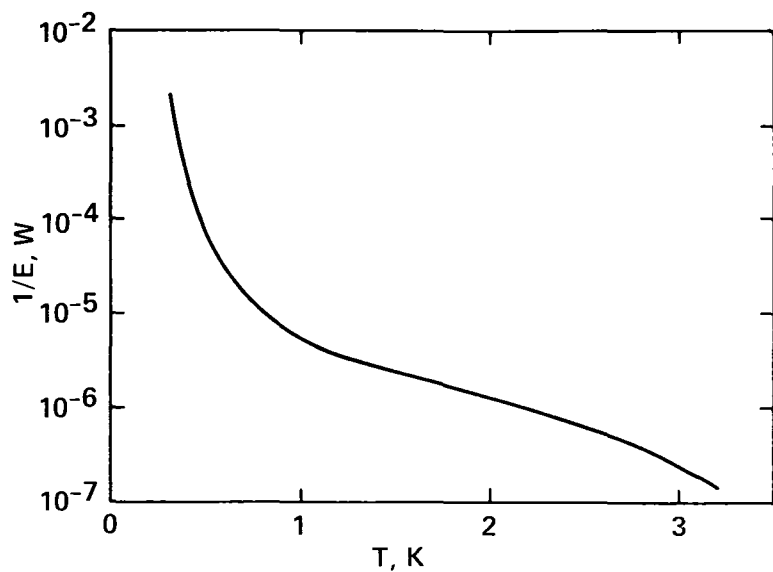


Figure 7.- Plot of $1/E_1$ as a function of temperature where it has been assumed that half of the thermal conductivity path is through copper and half is through ^3He .

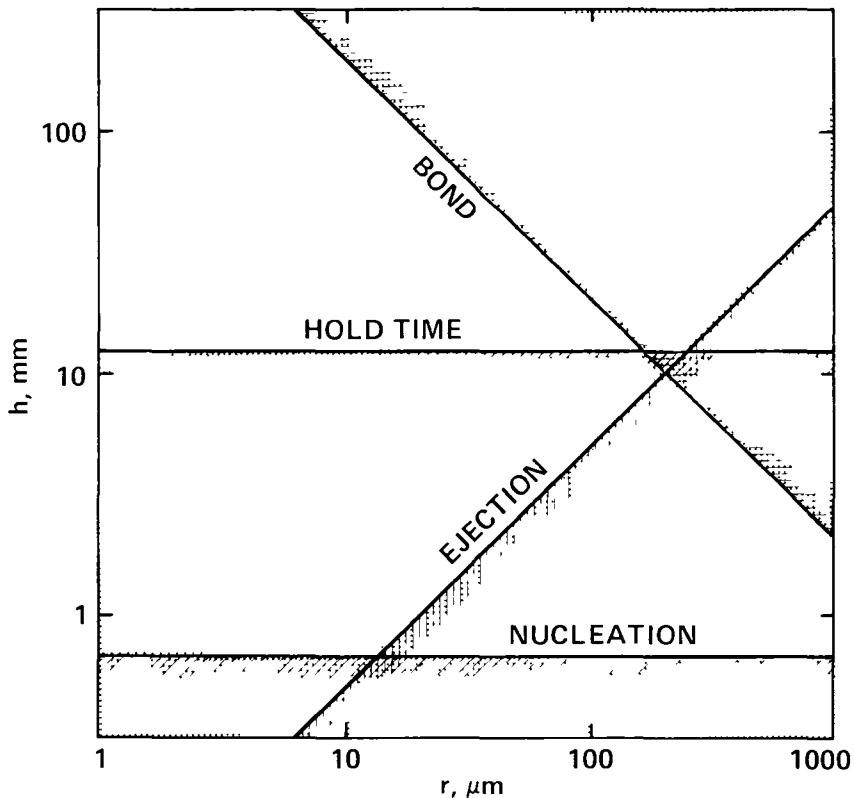


Figure 8.- Plot showing the stable and unstable regions of r - h space for various types of instabilities. The shading indicates the region of instability.

1 Report No NASA TM-85973	2 Government Accession No	3 Recipient's Catalog No	
4 Title and Subtitle DESIGN CONSIDERATIONS FOR A ³ HE REFRIGERATOR FOR SPACE APPLICATIONS		5 Report Date July 1984	6 Performing Organization Code
7 Author(s) Peter Kittel and Andres F. Rodriguez (University of the Pacific, Stockton, CA 95211)		8 Performing Organization Report No A-9786	10 Work Unit No T-6624
9 Performing Organization Name and Address Ames Research Center Moffett Field, CA 94035		11 Contract or Grant No	13 Type of Report and Period Covered Technical Memorandum
12 Sponsoring Agency Name and Address National Aeronautics and Space Administration Washington, DC 20546		14 Sponsoring Agency Code 506-54-21	
15 Supplementary Notes Point of Contact: Peter Kittel, Ames Research Center, M/S 244-7, Moffett Field, CA 94035 (415) 965-6525 or FTS 448-6525			
16 Abstract <p>The low temperature provided by ³He refrigerators (0.3-3 K) have useful space applications. However, the low temperatures and the low surface tension of ³He require special design considerations. These considerations include the need for small pores to contain the liquid in a matrix, the effects of bubble nucleation and growth, and the effects of the thermal conductivity within the matrix. These design considerations are discussed here along with an analysis of a possible confinement system.</p>			
17 Key Words (Suggested by Author(s)) Helium-3 Cryogenics Refrigeration		18 Distribution Statement Unlimited	
		Subject Category - 34	
19 Security Classif (of this report) Unclassified	20 Security Classif (of this page) Unclassified	21 No of Pages 21	22 Price* A02

End of Document